

A Bose-Einstein Condensate in a Uniform Light-induced Vector Potential

Y.-J. Lin, R. L. Compton, A. R. Perry, W. D. Phillips, J. V. Porto, and I. B. Spielman
National Institute of Standards and Technology, Gaithersburg, MD 20899

(Dated: October 24, 2018)

We use a two-photon dressing field to create an effective vector gauge potential for Bose-condensed ^{87}Rb atoms in the $F = 1$ hyperfine ground state. The dressed states in this Raman field are spin and momentum superpositions, and we adiabatically load the atoms into the lowest energy dressed state. The effective Hamiltonian of these neutral atoms is like that of charged particles in a uniform magnetic vector potential, whose magnitude is set by the strength and detuning of Raman coupling. The spin and momentum decomposition of the dressed states reveals the strength of the effective vector potential, and our measurements agree quantitatively with a simple single-particle model. While the uniform effective vector potential described here corresponds to zero magnetic field, our technique can be extended to non-uniform vector potentials, giving non-zero effective magnetic fields.

Ultracold atoms are an appealing system for the study of many-body correlated states relevant to condensed matter physics. These widely tunable systems in nearly disorder-free potentials have already realized one-dimensional Tonks-Girardeau gases [1], and the superfluid to Mott-insulator transition of a Bose-Einstein condensate (BEC) in an optical lattice [2]. The implementation of these simple iconic condensed matter systems paves the way for more interesting systems with exotic correlations and excitations, as in the fractional quantum Hall effect (FQHE) of a two-dimensional electron system in a strong magnetic field [3]. Simulating such a system with neutral atoms requires an effective Lorentz force, which is associated with a vector gauge potential. Current experimental approaches involve rotation of trapped BECs [4, 5], where low field effects, such as the formation of an Abrikosov vortex lattice, have been observed. For technical reasons, this approach is limited to modest effective fields, too small for FQHE physics [5, 6]. Most recent proposals to create significantly larger effective magnetic fields without rotation [7, 8, 9, 10, 11] involve optical coupling between internal atomic states, where the atoms are dressed in a spatially dependent manner. The effective magnetic field in such light-induced gauge potentials can be understood as a consequence of changing into a spatially varying basis of internal states. This is similar to the effective magnetic field in a rotating BEC arising from changing into the frame rotating with the BEC.

Here we report a first step toward using light-induced vector potentials to simulate magnetic fields. By dressing a BEC with two counter-propagating Raman laser beams, we realize a spatially uniform vector gauge potential. The Raman beams couple internal (spin) states with linear momenta differing by twice the photon momentum. This gives rise to a spatial gradient (along the Raman beam direction) of the phase difference between spin components of the dressed state. As we will show, this spatially varying state leads to a non-zero vector potential when the coupling is detuned from Raman resonance. We adiabatically load the BEC into the dressed state, and measure properties of the dressed-state disper-

sion relation by probing its spin and momentum decomposition. Although the atoms are stationary in the lab frame (having zero group velocity), the momenta of the individual spin components composing the dressed state show a non-zero phase velocity which depends on the strength and detuning of the Raman coupling. Our measurements agree with a simple single-particle model, and demonstrate the presence of an effective vector potential.

We dress a ^{87}Rb BEC in the $F=1$ ground state with two Raman laser beams counter-propagating along \hat{x} . Together these beams couple states $|m_F, k_x\rangle$ differing in internal angular momentum by \hbar ($\Delta m_F = \pm 1$), and differing in linear momentum k_x by $2k_r$. Here, $k_r = 2\pi/\lambda$ is the single-photon recoil momentum, and λ is the wavelength of the Raman beams. We define $E_r = \hbar^2 k_r^2 / 2m$ as the recoil energy. The family of three states coupled by the Raman field, $\Psi(\tilde{k}_x) = \{|-1, \tilde{k}_x + 2k_r\rangle, |0, \tilde{k}_x\rangle, |1, \tilde{k}_x - 2k_r\rangle\}$, are labeled by the quasi-momentum, \tilde{k}_x . The Raman beams have frequencies of ω_L and $(\omega_L + \Delta\omega_L)$ ($\Delta\omega_L > 0$), and a bias field $B_0 \hat{y}$ produces a Zeeman shift $\hbar\omega_Z = g\mu_B B_0 \simeq \hbar\Delta\omega_L$ (see Fig. 1ab). Since the momentum transfer is only along \hat{x} , the single-particle Hamiltonian can be written as $\mathcal{H} = \mathcal{H}_1(k_x) + [\hbar^2(k_y^2 + k_z^2)/2m + V(\vec{r})] \otimes \mathbf{1}$, where \mathcal{H}_1 is the Hamiltonian for the Raman coupling, the Zeeman energies and the motion along \hat{x} , and $\mathbf{1}$ is the 3×3 unit matrix acting on the spin space. $V(\vec{r})$ is the state-independent trapping potential (arising from a far-off-resonance dipole trap and the scalar light shift of the Raman beams), and m is the atomic mass. In the rotating wave approximation for the frame rotating at $\Delta\omega_L$, \mathcal{H}_1/\hbar expressed in the state basis of the family $\Psi(\tilde{k}_x)$ is

$$\begin{pmatrix} \frac{\hbar}{2m}(\tilde{k}_x + 2k_r)^2 - \delta & \Omega_R/2 & 0 \\ \Omega_R/2 & \frac{\hbar}{2m}\tilde{k}_x^2 - \epsilon & \Omega_R/2 \\ 0 & \Omega_R/2 & \frac{\hbar}{2m}(\tilde{k}_x - 2k_r)^2 + \delta \end{pmatrix}.$$

Here $\delta = (\Delta\omega_L - \omega_Z)$ is the detuning from Raman resonance, Ω_R is the resonant Raman Rabi frequency, and ϵ accounts for a small quadratic Zeeman shift (Fig. 1b). For each \tilde{k}_x , diagonalizing \mathcal{H}_1 gives three energy eigenvalues $E_j(\tilde{k}_x)$ ($j = 1, 2, 3$). For dressed atoms in state j ,

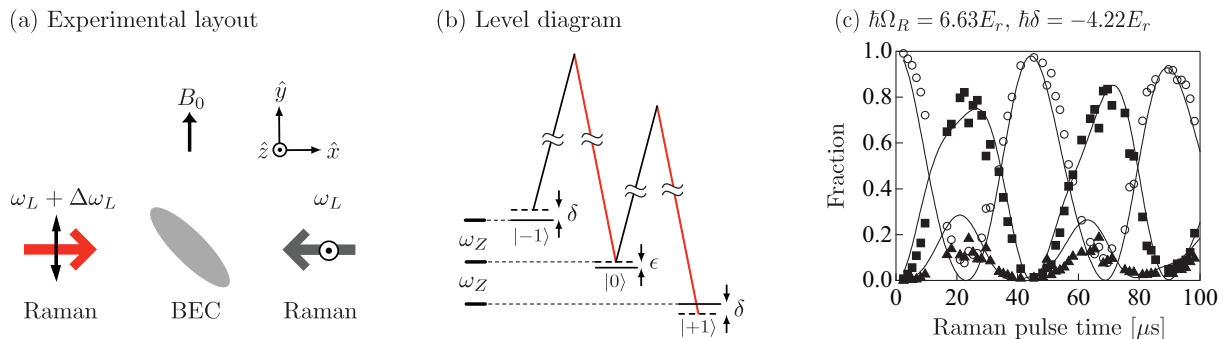


FIG. 1: (a) The ^{87}Rb BEC in a dipole trap created by two 1550 nm crossed beams in a bias field $B_0\hat{y}$ (gravity is along $-\hat{z}$). The two Raman laser beams are counter-propagating along \hat{x} , with frequencies ω_L and $(\omega_L + \Delta\omega_L)$, linearly polarized along \hat{z} and \hat{y} , respectively. (b) Level diagram of Raman coupling within the $F = 1$ ground state. The linear and quadratic Zeeman shifts are ω_Z and ϵ , and δ is the Raman detuning. (c) As a function of Raman pulse time, we show the fraction of atoms in $|m_F = -1, k_x = 0\rangle$ (open circles), $|0, -2k_r\rangle$ (solid squares), and $|+1, -4k_r\rangle$ (solid triangles), the states comprising the $\Psi(\tilde{k}_x = -2k_r)$ family. The atoms start in $| -1, k_x = 0\rangle$, and are nearly resonant for the $| -1, 0\rangle \rightarrow |0, -2k_r\rangle$ transition at $\hbar\delta = -4.22E_r$. We determine $\hbar\Omega_R = 6.63(4)E_r$ by a global fit (solid lines) to the populations in $\Psi(-2k_r)$.

$E_j(\tilde{k}_x)$ is the effective dispersion relation, which depends on experimental parameters, δ , Ω_R , and ϵ (left panels of Fig. 2). For example, the number of energy minima (from one to three) and their positions, \tilde{k}_{min} , are experimentally tunable. Around each \tilde{k}_{min} , the dispersion can be expanded as $E(\tilde{k}_x) \approx \hbar^2(\tilde{k}_x - \tilde{k}_{\text{min}})^2/2m^*$, where m^* is an effective mass. In this expansion, we identify \tilde{k}_{min} with the light-induced vector gauge potential, in analogy to the Hamiltonian for a particle of charge q in the usual magnetic vector potential \vec{A} : $(\vec{p} - q\vec{A})^2/2m$. In our experiment, we load a trapped BEC into the lowest energy $j = 1$ dressed state, and measure its quasi-momentum, equal to \tilde{k}_{min} for adiabatic loading.

Our experiment starts with a 3D ^{87}Rb BEC in a combined magnetic-quadrupole plus optical trap, as described in Ref. [12]. We transfer the atoms to an all-optical crossed dipole trap, formed by a pair of 1550 nm beams, by ramping the quadrupole field gradient to zero. The trapping beams are aligned along $\hat{x} - \hat{y}$ (horizontal beam) and at $\sim 10^\circ$ from \hat{z} (vertical beam). A uniform bias field along \hat{y} gives a linear Zeeman shift $\omega_Z/2\pi \simeq 3.25$ MHz and a quadratic shift $\epsilon/2\pi = 1.55$ kHz. The optically-trapped condensate typically has $N = 2.5 \times 10^5$ atoms in $|m_F = -1, k_x = 0\rangle$, with measured trap frequencies of ≈ 30 Hz parallel to, and ≈ 95 Hz perpendicular to, the horizontal beam.

In order to Raman-couple states differing in m_F by ± 1 , the $\lambda = 804.3$ nm Raman beams are linearly polarized along \hat{y} and \hat{z} , corresponding to π and σ relative to the quantization axis \hat{y} . The beams have $1/e^2$ radii of $180(20) \mu\text{m}$ [15], much larger than the $20 \mu\text{m}$ BEC. These beams give a total scalar light shift up to $60E_r$, where $E_r = h \times 3.55$ kHz, and contribute an additional harmonic potential with frequency up to 50 Hz along \hat{y} and \hat{z} . The differential light shift between adjacent m_F

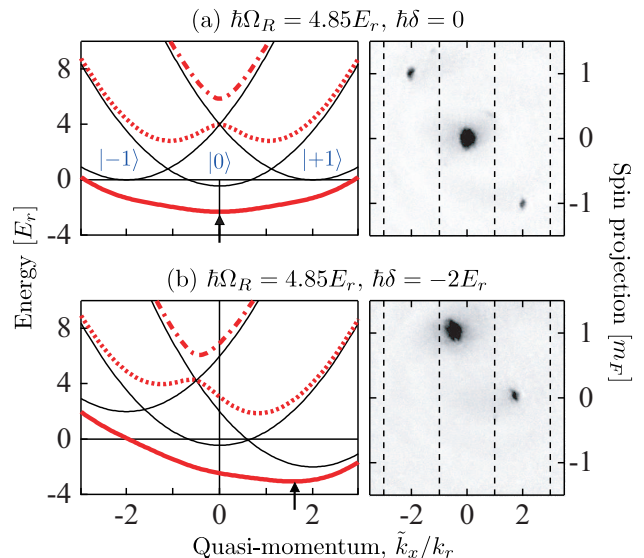


FIG. 2: Left panels: Energy-momentum dispersion curves $E(\tilde{k}_x)$ for $\hbar\epsilon = 0.44E_r$ and detuning $\hbar\delta = 0$ in (a) and $\hbar\delta = -2E_r$ in (b). The thin solid curves denote the three states $| -1, \tilde{k}_x + 2k_r\rangle$, $|0, \tilde{k}_x\rangle$, $|+1, \tilde{k}_x - 2k_r\rangle$ in absence of Raman coupling; the thick solid, dotted and dash-dotted curves indicate dressed states at Raman Rabi frequency $\Omega_R = 4.85E_r/\hbar$. The arrows indicate $\tilde{k}_x = \tilde{k}_{\text{min}}$ in the $j = 1$ dressed state. Right panels: Time-of-flight images of the Raman-dressed state at $\hbar\Omega_R = 4.85(35)E_r$, for detuning $\hbar\delta = 0$ in (a), and $\hbar\delta = -2E_r$ in (b). The Raman beams are along \hat{x} , and the three spin and momentum components, $| -1, \tilde{k}_{\text{min}} + 2k_r\rangle$, $|0, \tilde{k}_{\text{min}}\rangle$ and $|+1, \tilde{k}_{\text{min}} - 2k_r\rangle$, are separated along \hat{y} (after a small shear in the image which realigns the Stern-Gerlach gradient direction along \hat{y}).

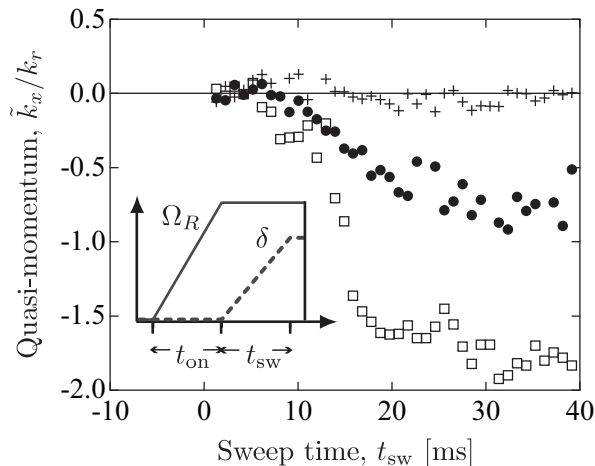


FIG. 3: Quasi-momentum \tilde{k}_x of the Raman-dressed state versus sweeping time t_{sw} of Raman detuning from $\hbar\delta = 0$ to $\hbar\delta = 1E_r$ (solid circles) and $\hbar\delta = 2E_r$ (open squares), at $\hbar\Omega_R = 5E_r$. The crosses denote $\tilde{k}_x = 0$ without sweeping ($\hbar\delta = 0$). The inset shows the time sequence of Ω_R and δ for the loading into a detuned Raman-dressed state.

states arising from the combination of misalignment and imperfect polarization is estimated to be smaller than $0.2E_r$. We determine Ω_R by observing population oscillations driven by the Raman beams and fitting to the expected behavior, as shown in Fig. 1c.

We developed a procedure to adiabatically load the $|-1, k_x = 0\rangle$ BEC into the lowest energy, $j = 1$, Raman-dressed state. For a BEC initially in $|0, k_x = 0\rangle$, this could be achieved simply by slowly turning on the Raman beams at detuning $\delta = 0$, resulting in the $j = 1$, $\tilde{k}_x = 0$ dressed state, located at the minimum of $E_{j=1}(\tilde{k}_x)$. However, our initial state $|-1, k_x = 0\rangle$, for which $k_x = \tilde{k}_x + 2k_r$, is a member of the family of states $\Psi(\tilde{k}_x = -2k_r)$. This simple loading procedure would therefore result in the $j = 1$, $\tilde{k}_x = -2k_r$ dressed state. In order to transfer our $\tilde{k}_x = -2k_r$ BEC to the desired $\tilde{k}_x = 0$ dressed state, we use an additional rf coupling which mixes families of states with \tilde{k}_x differing by $2k_r$. The rf frequency is always equal to the frequency difference between two Raman beams, $\Delta\omega_L/2\pi = 3.250$ MHz. The loading sequence is as follows: (i) We turn on the rf coupling in 1 ms to a resonant Rabi frequency $\Omega_{rf}/2\pi = 12$ kHz, with an initial detuning $\hbar\delta = 15E_r$. We then sweep the detuning to resonance [16] in 9 ms (δ is varied by ramping the bias field B_0 , leaving $\Delta\omega_L$ constant.), loading the atoms into the lowest energy rf-dressed state, a spin superposition still at $k_x = 0$. (ii) We ramp on the Raman coupling in $t_{on} = 20$ ms to a variable Rabi frequency Ω_R , and then turn off the rf in 2 ms. This loads the BEC into the $j = 1$, $\tilde{k}_x = 0$ dressed state. In the dressed state, the BEC heats at ~ 0.3 nK/ms, we believe due to technical noise in B_0 or $\Delta\omega_L$. In addition, we observe unwanted population in the $j = 2$ dressed state.

Therefore, as part of step (ii), we further evaporatively cool by decreasing the intensity of the horizontal trapping beam by 20% in 20 ms, after which it remains constant. The evaporation typically reduces the BEC number to 7×10^4 .

In the final step (iii), we transfer the $\tilde{k}_x = 0$ dressed state into a non-zero \tilde{k}_x state by sweeping the detuning from resonance to a variable δ in t_{sw} and holding for t_h . As we show below, for $t_{sw} \gtrsim 20$ ms, this process adiabatically loads the atoms into the $j = 1$ Raman-dressed state at $\tilde{k}_x = \tilde{k}_{min}(\delta)$.

We characterize the Raman-dressed state by abruptly turning off the dipole trap and the Raman beams in less than $1 \mu\text{s}$, projecting the atomic state onto its individual spin and momentum components. The atoms then expand in a magnetic field gradient applied during time-of-flight (TOF) approximately along \hat{y} , and the three spin states spatially separate due to the Stern-Gerlach effect. Imaging the atoms after a 20 ms TOF gives the momentum and spin composition of the dressed state (see right panels of Fig. 2). The quasi-momentum \tilde{k}_x of the BEC is given by the shift along \hat{x} of all three spin components from their positions when $\tilde{k}_x = 0$. We determine $\tilde{k}_x = 0$ to within $0.03 k_r$ by using the loading procedure above, except that in (ii), the Raman frequencies are sufficiently far-detuned that the atoms experience the scalar light shift but are not Raman-coupled; then the rf and Raman fields are snapped off concurrently before TOF.

It is straightforward to adiabatically load into the rf-dressed state in step (i). To ensure the subsequent adiabatic loading from the rf-dressed state into the Raman-dressed state in step (ii), we ramped up the Raman power in a time t_{on} , then ramped it off in t_{on} . For $t_{on} \geq 2$ ms, there is no discernable excitation into other rf-dressed states. We conservatively use $t_{on} = 20$ ms as the loading time in step (ii). To determine t_{sw} in step (iii), we measure \tilde{k}_x as a function of t_{sw} for negligible t_h . Figure 3 shows \tilde{k}_x versus t_{sw} at $\hbar\delta = 0, 1, 2E_r$ and $\hbar\Omega_R = 5E_r$, for $t_h = 0.1$ ms. We use $t_{sw} = 20$ ms, the time at which \tilde{k}_x has nearly reached its equilibrium value. This adiabatic following is enabled by the external trap, and the time scale is comparable to our typical trapping periods. After t_{sw} , we add a hold time $t_h = 20$ ms during which residual excitations damp.

Figure 2 shows spin-resolved TOF images of adiabatically loaded Raman-dressed states at $\hbar\Omega_R = 4.85(35)E_r$ for $\hbar\delta = -2$ and $0E_r$. The resonance condition, $\delta = 0$, is determined from the symmetry of the rf-dressed state [17], with an uncertainty of $h \times 1.5$ kHz $= 0.4E_r$, limited by the stability of B_0 . The quasi-momentum $\tilde{k}_x = \tilde{k}_{min}$, measured as a function of δ , is shown in Fig. 4a, along with the calculated $\tilde{k}_{min}(\delta)$. Each different \tilde{k}_{min} represents a spatially uniform vector gauge potential, analogous to the magnetic vector potential, with $\tilde{k}_{min} = q\vec{A}/\hbar$. For such a uniform \vec{A} , the magnetic field $\vec{B} = \nabla \times \vec{A}$ would be zero.

For Rabi frequency $\Omega_R \leq 4.47E_r/\hbar$, $E_{j=1}(\tilde{k}_x)$ has mul-

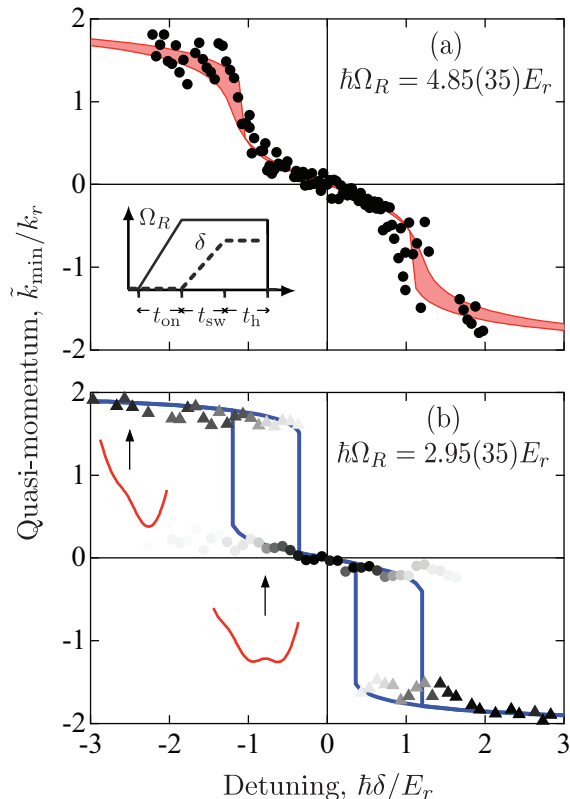


FIG. 4: (a) Measured quasi-momentum \tilde{k}_{\min} versus detuning δ , and the calculated \tilde{k}_{\min} at Rabi frequency $\Omega_R = 4.85(35)E_r/\hbar$ (with the uncertainty indicated by the shaded region). The inset shows the time sequence of Ω_R and δ . (b) Quasi-momentum $\tilde{k}_{\min 1}$ (circles) and $\tilde{k}_{\min 2}$ (triangles) versus detuning δ , and the calculated \tilde{k}_{\min} (solid lines) at $\hbar\Omega_R = 2.95(35)E_r$. The intensity of the circles indicates the population of $|0, \tilde{k}_{\min 1}\rangle$ relative to its value at $\delta = 0$. The intensity of the triangles for $\delta < 0$ ($\delta > 0$) indicates the population of $|+1, \tilde{k}_{\min 2} - 2k_r\rangle$ ($|-1, \tilde{k}_{\min 2} + 2k_r\rangle$) relative to its value at $\hbar\delta = -3E_r$ ($\hbar\delta = 3E_r$). The insets picture $E(\tilde{k}_x)$ at $\hbar\delta = -0.8$ and $-2.5E_r$ as indicated by the arrows.

multiple minima for some detunings δ . For data taken as in Fig. 4a, Fig. 4b shows such multiple \tilde{k}_{\min} , expected for $\delta_a < |\delta| < \delta_b$, where $\hbar\delta_a = 0.35(20)E_r$ and $\hbar\delta_b = 1.2(1)E_r$, at $\hbar\Omega_R = 2.95(35)E_r$. At small and large detuning, we observe only one \tilde{k}_{\min} . However, at intermediate detuning, we observe two \tilde{k}_{\min} at $\tilde{k}_{\min 1}$ and $\tilde{k}_{\min 2}$ [13]. In the figure, the relative population is indicated by the gray scale, and the solid line is the calculated value(s). The observed values of $\tilde{k}_{\min}(\delta)$ agree well with the theory, and a simultaneous fit of $\tilde{k}_{\min 1}$ and $\tilde{k}_{\min 2}$ with Ω_R as a free parameter gives $\hbar\Omega_R = 2.9(3)E_r$, which agrees well with the independently measured $\hbar\Omega_R = 2.95(35)E_r$. As expected, we observe population in only one \tilde{k}_x for $|\delta| < \delta_a$, however, for some $|\delta| > \delta_b$, there is discernable population in two \tilde{k}_x where we expect only one \tilde{k}_{\min} . We attribute this to non-adiabicity when the minimum at $\tilde{k}_{\min 1}$ disappears during the detuning sweep in loading step (iii).

In conclusion, we have prepared a Bose-Einstein condensate in a Raman-dressed state with a non-zero quasi-momentum, controlled by the Rabi frequency Ω_R and the detuning δ . This technique, in conjunction with a spatial gradient of the bias field (therefore the detuning) along \hat{y} , gives a spatial gradient of light-induced momentum $k_{\min}(y)\hat{x}$ and creates an effective magnetic field along \hat{z} [14]. The analog of the magnetic length $l_B = \sqrt{\hbar/(qB)}$ (the classical cyclotron radius of an orbit with one unit of angular momentum \hbar) is $(\partial\tilde{k}_{\min}/\partial y)^{-1/2}$, and is about the spacing between vortices in a vortex lattice like that formed in a slowly rotating BEC [5]. For a gradient in \tilde{k}_{\min} of one k_r across a condensate of radius R , this gives an analog magnetic length $\approx 1.4 \mu\text{m}$ for a $R \approx 10 \mu\text{m}$ 3D BEC, and we expect a ~ 25 -vortex lattice to form in the condensate. For dilute 2D systems, this is sufficient to reach the quantum Hall regime.

This work was partially supported by ONR, ODNI, and ARO with funds from the DARPA OLE program. R.L.C. acknowledges the NIST/NRC postdoctoral program.

-
- [1] B. Paredes, A. Widera, V. Murg, O. Mandel, S. Fölling, I. Cirac, G. V. Shlyapnikov, T. W. Hänsch, and I. Bloch, *Nature* **429**, 277 (2004); T. Kinoshita, T. Wenger, and D. Weiss, *Science* **305**, 1125 (2004).
- [2] M. Greiner, O. Mandel, T. Esslinger, T. W. Hänsch, and I. Bloch, *Nature* **415**, 39 (2002); T. Stöferle, H. Moritz, C. Schori, M. Köhl, and T. Esslinger, *Phys. Rev. Lett.* **92**, 130403 (2004); I. B. Spielman, W. D. Phillips, and J. V. Porto, *Phys. Rev. Lett.* **98**, 080404 (2007).
- [3] D. C. Tsui, H. L. Stormer, and A. C. Gossard, *Phys. Rev. Lett.* **48**, 1559 (1982); R. B. Laughlin, *Phys. Rev. Lett.* **50**, 1395 (1983).
- [4] J. R. Abo-Shaer, C. Raman, J. M. Vogels, and W. Ketterle, *Science* **292**, 476 (2001); V. Bretin, S. Stock, Y. Seurin, and J. Dalibard, *Phys. Rev. Lett.* **92**, 050403 (2004).
- [5] V. Schweikhard, I. Coddington, P. Engels, V. P. Mosen-dorff, and E. A. Cornell, *Phys. Rev. Lett.* **92**, 040404 (2004).
- [6] I. Bloch, J. Dalibard, and W. Zwerger, *Rev. Mod. Phys.* **80**, 885 (2008).
- [7] D. Jaksch and P. Zoller, *New J. Phys.* **5**, 56 (2003).
- [8] A. S. Sørensen, E. Demler, and M. D. Lukin, *Phys. Rev. Lett.* **94**, 086803 (2005); M. Hafezi, A. S. Sørensen, E. Demler, and M. D. Lukin, *Phys. Rev. A* **76**, 023613 (2007).
- [9] S.-L. Zhu, H. Fu, C.-J. Wu, S.-C. Zhang, and L.-M. Duan, *Phys. Rev. Lett.* **97**, 240401 (2006).

- [10] G. Juzeliūnas and P. Öhberg, Phys. Rev. Lett. **93**, 033602 (2004); G. Juzeliūnas, J. Ruseckas, P. Öhberg, and M. Fleischhauer, Phys. Rev. A **73**, 025602 (2006).
- [11] J. Higbie and D. M. Stamper-Kurn, Phys. Rev. Lett. **88**, 090401 (2002); F. Papoff, F. Mauri, and E. Arimondo, J. Opt. Soc. Am. B **9**, 321 (1992).
- [12] Y.-J. Lin, A. Perry, R. L. Compton, J. V. Porto, and I. B. Spielman, in preparation.
- [13] T. D. Stanescu, B. Anderson, and V. Galitski, Phys. Rev. A **78**, 023616 (2008).
- [14] I. B. Spielman, in preparation.
- [15] Uncertainties reflect the uncorrelated combination of $1\text{-}\sigma$ statistical and systematic uncertainties.
- [16] All the detuning ramps are linear versus time. The Raman beam power, swept by applying a linear ramp to the AOM controlling its power, turns on nearly quadratically.
- [17] On resonance the rf-dressed state has equal population in $|-1, k_x = 0\rangle$ and $|+1, k_x = 0\rangle$, even in the presence of a quadratic Zeeman shift. The resonance condition $\delta=0$ determined from the symmetry of the Raman dressing is within $0.25E_r$ of that from the rf-dressed states.